Arrangement for the K_2^* meson family

Ting-Yan Li,[1,2,3,*] Ya-Rong Wang,[4,2,3,†] and Cheng-Qun Pang[5,4,2,3,‡]

[1]*School of Physical Science and Technology, Lanzhou University, Lanzhou 730000, China*
[2]*Joint Research Center for Physics, Lanzhou University and Qinghai Normal University, Xining 810000, China*
[3]*Lanzhou Center for Theoretical Physics, Key Laboratory of Theoretical Physics of Gansu Province, Lanzhou University, Lanzhou, Gansu 730000, China*
[4]*College of Physics and Electronic Information Engineering, Qinghai Normal University, Xining 810000, China*
[5]*School of Physics Optoelectronic Engineering, Ludong University, Yantai 264000, China*

(Received 2 October 2022; accepted 21 February 2023; published 11 April 2023)

Two observed structures with $M = 1868 \pm 8^{+40}_{-57}$ MeV and $M = 2073 \pm 94^{+245}_{-240}$ MeV are the same states [$K_2^*(1980)$] in Particle Data Group. In this paper, analysis of the mass spectrum and calculation of the strong decay for K_2^* mesons support the assignment of 2^3P_2 and 1^3F_2 as the low- and high-mass states for $K_2^*(1980)$. This analysis reveals very important criteria for the assignment of the observed $K_2^*(1980)$, and experimental findings for this assignment are suggested. Additionally, some partial decay widths are predicted based on the high excitations of the K_2^* family. This study is crucial for establishing and searching for the higher excitations in the future.

DOI: 10.1103/PhysRevD.107.074008

I. INTRODUCTION

The K_2^* meson family is a crucial component of the kaon family. There are two members in this family of K_2^* mesons: $K_2^*(1430)$ and $K_2^*(1980)$. $K_2^*(1430)$ is well established as the ground state of the K_2^* meson family with a 1^3P_2 assignment. $K_2^*(1980)$ is now listed in Particle Data Group (PDG) [1] with an average mass and width of 1995^{+60}_{-50} MeV and 349^{+50}_{-30} MeV. The existence of $K_2^*(1980)$ as a 2^3P_2 or a 1^3F_2 state has aroused our attention.

The $K_2^*(1980)$ meson was reported by the LASS Collaboration in 1987 and 1989 in $K^- p \to \bar{K}^0\pi^+\pi^- n$ and $K^- p \to \bar{K}^0\pi^- p$ processes, whose mass is $1973 \pm 8 \pm 25$ MeV and corresponding width is $373 \pm 33 \pm 60$ MeV in 1989, the LASS Collaboration gave the resonance parameters of $K_2^*(1980)$ with $M = 1978 \pm 40$ MeV and $\Gamma = 398 \pm 47$ MeV, respectively) [1,2]. This meson is likely to be the candidate for the 2^3P_2 state or 1^3F_2 state.

Recently, the BESIII Collaboration observed $K_2^*(1980)$ in the $K\pi$ channel in the process $J/\psi \to K^+K^-\pi^0$. They obtained two solutions when fitting the experimental data, $M = 1817 \pm 11$ MeV and $\Gamma = 312 \pm 28$ MeV, or $M = 1868 \pm 8^{+40}_{-51}$ MeV and $\Gamma = 272 \pm 24^{+50}_{-15}$ MeV [3]. The mass of this meson is approximately 250 MeV lower than the value of $2073 \pm 94^{+245}_{-240}$ MeV detected by the LHCb Collaboration [4]. The resonances for $K_2^*(1980)$ were later provided by the LHCb Collaboration. They regarded $K_2^*(1980)$ as the 2^3P_2 state, where $J^P = 2^+$, the mass is of $1988 \pm 22^{+194}_{-31}$ MeV, and the width is of $318 \pm 82^{+481}_{-101}$ MeV [5]. Recent observations of $K_2^*(1980)$ by the BESIII Collaboration by means of partial-wave analysis of $\psi(3686) \to K^+K^-\eta$ also gave the resonance parameters $M = 2046^{+17+67}_{-16-15}$ MeV and $\Gamma = 408^{+38+72}_{-34-44}$ MeV [6]. Do these structures belong to the same state?

We contrast the a_2 and K_2 families in Fig. 1 to find the solution to this query. In the a_2 family, the mass difference between the 1^3P_2 and 2^3P_2 states is 388 MeV.

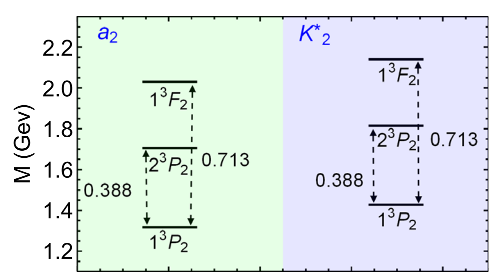

FIG. 1. Mass gap comparison between K_2^* and a_2 family. The left part of the figure is the mass gap of a_2 family and the right part of the figure is the mass gap of K_2^* family.

*litingyan1213@163.com
†nanoshine@foxmail.com
‡Corresponding author.
pcq@qhnu.edu.cn

Additionally, there is a mass gap of 713 MeV between the $1^3P_2(a_2(1320))$ and $1^3F_2(a_2(2030))$ states. If we put this mass gap into the K_2 family, and use 1427.3 MeV as the mass of the $1^3P_2(K_2^*(1430))$ state, then the mass of the 2^3P_2 state will be 1815.3 MeV, which is extremely close to the experimental value $M = 1817 \pm 11$ MeV (or solution two, $1868 \pm 8^{+40}_{-57}$ MeV) [1]. The mass of the 1^3F_2 state will be 2140.3 MeV, consistent with $2073 \pm 94^{+245}_{-240}$ MeV [1]. Following this analysis, the structure with $M = 1817 \pm 11$ MeV (or the second solution $1868 \pm 8^{+40}_{-57}$ MeV, which, in this work, we name $K_2^*(1870)$) [1] should be the 2^3P_2 state and the state with $M = 2073 \pm 94^{+245}_{-240}$ MeV [1] [which, in this work, we name $K_2^*(2070)$] could be the $K_2^*(1^3F_2)$ state.

To test the proposed assignment of $K_2^*(1870)$ and $K_2^*(2070)$, in the following, we determine the mass and decay width for $K_2^*(2^3P_2)$ and $K_2^*(1^3F_2)$ via the mass spectrum and two-body strong decay of K_2^*. At the same time, the property of the higher excited K_2^* states will be investigated.

Godfrey and Isgur proposed the GI model for describing relativistic meson spectra in 1985 [7]. The screened effect was demonstrated by the lattice calculations [8–11], which stimulated the study of the quark-quark interaction in the works [12–14]. References [15,16] discussed the relation between the coupled-channel effect with intermediate meson-meson loops and the screened effect. Song *et al.* developed the modified GI (MGI) model taking into account the screened effect in the GI model [17,18]. In this work, we study the mass spectra for K_2^* mesons more preferably with the help of MGI model considering this phenomenological screened potential. In fact, the interaction energy obtained by lattice-field theoretic computations is not a potential; rather, it reveals the adiabatic crossing of two potentials, one for a heavy quark-antiquark system, and one for a meson-meson system [8–11]. Indeed, integrating out the continuum channel gives rise to a short-distance correction to the quark-antiquark interaction, not a long-distance one. Thus, there is no reason to believe that the total energy of kaon system goes to a maximum value of 3.72 GeV when $r \to \infty$ [19].

The spatial wave functions obtained by the modified GI model can be taken as input when we study the K_2^* family's Okubo-Zweig-Iizuka (OZI)-allowed two-body strong decays adopting the quark-pair creation (QPC) model, which was proposed in Ref. [20] and extensively applied to studies of other hadrons in Refs. [21–47].

This paper is organized as follows. After the Introduction, in Sec. II, we explain the modified Godfrey-Isgur model and the QPC model. In Sec. III, we adopt the modified Godfrey-Isgur model by including the screened effect to study the mass spectra obtained for the K_2^* family. We further obtain the structural information for the observed K_2^* via making a comparison between theoretical and experimental results. We present a detailed study of the OZI-allowed two-body strong decays of the discussed kaons. The paper ends with a conclusion.

II. PHENOMENOLOGICAL ANALYSIS OF K_2^* MESONS

In this work, the modified GI quark model is utilized to calculate the mass spectrum and wave functions for the K_2^* meson family. We also investigated the two-body strong decay of the K_2^* meson family with the QPC model. In the following, these models will be illustrated in detail.

A. Brief review of the MGI and QPC models

1. MGI model

Godfrey and Isgur proposed the GI model for describing relativistic meson spectra with great success, exactly for low-lying mesons [7]. For excited states, the screened potential must be taken into account for coupled-channel effect [48–50].

The interaction between the quark and antiquark is depicted by the Hamiltonian of the potential model, including the kinetic energy and effective potential,

$$\tilde{H} = \sqrt{m_1^2 + \mathbf{p}^2} + \sqrt{m_2^2 + \mathbf{p}^2} + \tilde{V}_{\mathrm{eff}}(\mathbf{p}, \mathbf{r}), \qquad (1)$$

where m_1 and m_2 denote the mass of the quark and antiquark, respectively, and the effective potential $\tilde{V}_{\mathrm{eff}}$ contains two ingredients, a short-range $\gamma^\mu \otimes \gamma_\mu$ one-gluon-exchange interaction and a $1 \otimes 1$ linear confinement interaction. The meaning of the tilde will be explained later.

In the nonrelativistic limit, the effective potential has a familiar format [7,51]:

$$V_{\mathrm{eff}}(r) = H^{\mathrm{conf}} + H^{\mathrm{hyp}} + H^{\mathrm{so}}, \qquad (2)$$

with

$$\begin{aligned} H^{\mathrm{conf}} &= \left[-\frac{3}{4}(br + c) + \frac{\alpha_s(r)}{r}\right](\boldsymbol{F}_1 \cdot \boldsymbol{F}_2) \\ &= S(r) + G(r), \end{aligned} \qquad (3)$$

$$\begin{aligned} H^{\mathrm{hyp}} = -\frac{\alpha_s(r)}{m_1 m_2}\Bigg[&\frac{8\pi}{3}\boldsymbol{S}_1 \cdot \boldsymbol{S}_2 \delta^3(\boldsymbol{r}) \\ &+ \frac{1}{r^3}\left(\frac{3\boldsymbol{S}_1 \cdot \boldsymbol{r}\boldsymbol{S}_2 \cdot \boldsymbol{r}}{r^2} - \boldsymbol{S}_1 \cdot \boldsymbol{S}_2\right)\Bigg](\boldsymbol{F}_1 \cdot \boldsymbol{F}_2), \end{aligned} \qquad (4)$$

$$H^{\mathrm{so}} = H^{\mathrm{so(cm)}} + H^{\mathrm{so(tp)}}, \qquad (5)$$

where H^{conf} includes the spin-independent linear confinement piece $S(r)$ and Coulomb-like potential from one-gluon-exchange $G(r)$. H^{hyp} denotes the color-hyperfine interaction consisting of tensor and contact terms. H^{SO} is the spin-orbit interaction with

$$H^{\mathrm{so(cm)}} = \frac{-\alpha_s(r)}{r^3}\left(\frac{1}{m_1}+\frac{1}{m_2}\right)\left(\frac{\boldsymbol{S}_1}{m_1}+\frac{\boldsymbol{S}_2}{m_2}\right)\cdot \boldsymbol{L}(\boldsymbol{F}_1\cdot\boldsymbol{F}_2), \tag{6}$$

which is caused by one-gluon exchange and

$$H^{\mathrm{so(tp)}} = -\frac{1}{2r}\frac{\partial H^{\mathrm{conf}}}{\partial r}\left(\frac{\boldsymbol{S}_1}{m_1^2}+\frac{\boldsymbol{S}_2}{m_2^2}\right)\cdot\boldsymbol{L}, \tag{7}$$

which is the Thomas precession term.

For the above formulas, $\boldsymbol{S}_1/\boldsymbol{S}_2$ indicates the spin of the quark/antiquark and $\boldsymbol{L}$ is the orbital momentum between the two particles. $\boldsymbol{F}$ is relevant to the Gell-Mann matrix, i.e., $\boldsymbol{F}_1=\boldsymbol{\lambda}_1/2$ and $\boldsymbol{F}_2=-\boldsymbol{\lambda}_2^*/2$, and for a meson, $\langle\boldsymbol{F}_1\cdot\boldsymbol{F}_2\rangle=-4/3$.

Now the relativistic effects of distinguishing influence must be considered especially in meson systems, which are embedded in two different ways. First, based on the nonlocal interactions and new $\mathbf{r}$ dependence, a smearing function is introduced for a meson $q\bar{q}$:

$$\rho(\mathbf{r}-\mathbf{r}') = \frac{\sigma^3}{\pi^{3/2}}e^{-\sigma^2(\mathbf{r}-\mathbf{r}')^2}, \tag{8}$$

which is applied to $S(r)$ and $G(r)$ to obtain smeared potentials $\tilde{S}(r)$ and $\tilde{G}(r)$ by

$$\tilde{f}(r) = \int d^3\mathbf{r}'\rho(\mathbf{r}-\mathbf{r}')f(r'), \tag{9}$$

with

$$\sigma_{12}^2 = \sigma_0^2\left[\frac{1}{2}+\frac{1}{2}\left(\frac{4m_1m_2}{(m_1+m_2)^2}\right)^4\right]+s^2\left(\frac{2m_1m_2}{m_1+m_2}\right)^2. \tag{10}$$

Second, owing to relativistic effects, a general potential should rely on the center of mass of the interacting quarks. Momentum-dependent factors that will be unity in the nonrelativistic limit are applied as

$$\tilde{G}(r)\to\left(1+\frac{p^2}{E_1E_2}\right)^{1/2}\tilde{G}(r)\left(1+\frac{p^2}{E_1E_2}\right)^{1/2}, \tag{11}$$

and

$$\frac{\tilde{V}_i(r)}{m_1m_2}\to\left(\frac{m_1m_2}{E_1E_2}\right)^{1/2+\epsilon_i}\frac{\tilde{V}_i(r)}{m_1m_2}\left(\frac{m_1m_2}{E_1E_2}\right)^{1/2+\epsilon_i}, \tag{12}$$

where $\tilde{V}_i(r)$ represents the contact, tensor, vector spin-orbit, and scalar spin-orbit terms, and ϵ_i is the relevant modification parameter.

The screened effect can be introduced by the transformation $br+c\to\frac{b(1-e^{-\mu r})}{\mu}+c$, where μ is the screened parameter whose particular value is given by Ref. [19]. The modified confinement potential also requires similar relativistic correction, which has been mentioned in the GI model. Then, we further write

$$\begin{aligned}\tilde{V}^{\mathrm{scr}}(r) &= \int d^3\mathbf{r}'\rho(\mathbf{r}-\mathbf{r}')\frac{b(1-e^{-\mu r'})}{\mu}\\ &= \frac{b}{\mu r}\left[r+e^{\frac{\mu^2}{4\sigma^2}+\mu r}\frac{\mu+2r\sigma^2}{2\sigma^2}\left(\frac{1}{\sqrt{\pi}}\int_0^{\frac{\mu+2r\sigma^2}{2\sigma}}e^{-x^2}dx-\frac{1}{2}\right)\right.\\ &\quad\left.-e^{\frac{\mu^2}{4\sigma^2}-\mu r}\frac{\mu-2r\sigma^2}{2\sigma^2}\left(\frac{1}{\sqrt{\pi}}\int_0^{\frac{\mu-2r\sigma^2}{2\sigma}}e^{-x^2}dx-\frac{1}{2}\right)\right].\end{aligned} \tag{13}$$

The mass spectrum and the wave function for K_2^* mesons can be obtained by solving eigenvalue and eigenvector of the $\tilde{H}$ in Eq. (1) with the simple harmonic oscillator (SHO) base-expanding method. In configuration and momentum space, SHO wave functions have explicit forms, respectively,

$$\begin{aligned}\Psi_{nLM_L}(\mathbf{r}) &= R_{nL}(r,\beta)Y_{LM_L}(\Omega_r),\\ \Psi_{nLM_L}(\mathbf{p}) &= R_{nL}(p,\beta)Y_{LM_L}(\Omega_p),\end{aligned} \tag{14}$$

with

$$\begin{aligned}R_{nL}(r,\beta) &= \beta^{3/2}\sqrt{\frac{2n!}{\Gamma(n+L+3/2)}}(\beta r)^L e^{\frac{-r^2\beta^2}{2}}\\ &\quad\times L_n^{L+1/2}(\beta^2r^2),\end{aligned} \tag{15}$$

$$\begin{aligned}R_{nL}(p,\beta) &= \frac{(-1)^n(-i)^L}{\beta^{3/2}}e^{-\frac{p^2}{2\beta^2}}\sqrt{\frac{2n!}{\Gamma(n+L+3/2)}}\left(\frac{p}{\beta}\right)^L\\ &\quad\times L_n^{L+1/2}\left(\frac{p^2}{\beta^2}\right),\end{aligned} \tag{16}$$

where $Y_{LM_L}(\Omega)$ is the spherical harmonic function, and $L_{n-1}^{L+1/2}(x)$ is the associated Laguerre polynomial.

2. QPC model

The QPC model was first proposed by Micu [20], and was further developed by the Orsay group [21,52–55]. It was widely applied to the OZI-allowed two-body strong decay of hadrons in Refs. [22,23,26,28,30,32–37,40–43,45,46,56–61].

The decay process $A\to B+C$ can be expressed as follows:

$$\langle BC|\mathcal{T}|A\rangle = \delta^3(\mathbf{P}_B+\mathbf{P}_C)\mathcal{M}^{M_{J_A}M_{J_B}M_{J_C}}, \tag{17}$$

where $\mathbf{P}_{B(C)}$ is the three-momentum for a meson $B(C)$ in the rest frame of a meson A. The superscript M_{J_i}

TABLE I. Spectrum for the K_2^* meson family, where Exp. represent the experimental data [65]. Unit of mass is MeV.

State	Ref. [19]	Ref. [63]	GI [7]	Ebert [64]	Exp.
1^3P_2	1450	1432	1409	1424	1427 ± 1.5
2^3P_2	1906	1870	1924	1896	$1868 \pm 8^{+40}_{-51}$
3^3P_2	2274	2198	2370	...	...
4^3P_2	2570	2438	2756	...	...
1^3F_2	2200	2092	2168	1.964	$2073 \pm 94^{+245}_{-240}$
2^3F_2	2415	2356	2565	...	...
3^3F_2	2682	2552	2917	...	...

$(i = A, B, C)$ denotes an orbital magnetic momentum. The transition operator $\mathcal{T}$ is introduced to describe a quark-antiquark pair creation from vacuum, which has the quantum number $J^{PC} = 0^{++}$, $\mathcal{T}$ can be written as

$$\mathcal{T} = -3\gamma \sum_m \langle 1m; 1-m|00\rangle \int d\mathbf{p}_3 d\mathbf{p}_4 \delta^3(\mathbf{p}_3 + \mathbf{p}_4) \times \mathcal{Y}_{1m}\left(\frac{\mathbf{p}_3 - \mathbf{p}_4}{2}\right) \chi^{34}_{1,-m} \phi^{34}_0 (\omega^{34}_0)_{ij} b^\dagger_{3i}(\mathbf{p}_3) d^\dagger_{4j}(\mathbf{p}_4), \quad (18)$$

which is the transition operator and it can describe the creation of a quark-antiquark pair from vacuum, where the quark and antiquark are denoted by the indices 3 and 4, respectively. The parameter γ depicts the strength of the creation of $q\bar{q}$ from vacuum. $\mathcal{Y}_{\ell m}(\mathbf{p}) = |\mathbf{p}|^\ell Y_{\ell m}(\mathbf{p})$ are the solid harmonics. χ, ϕ, and ω denote the spin, flavor, and color wave functions, respectively, which can be treated separately. The subindices i and j denote the color of a $q\bar{q}$ pair.

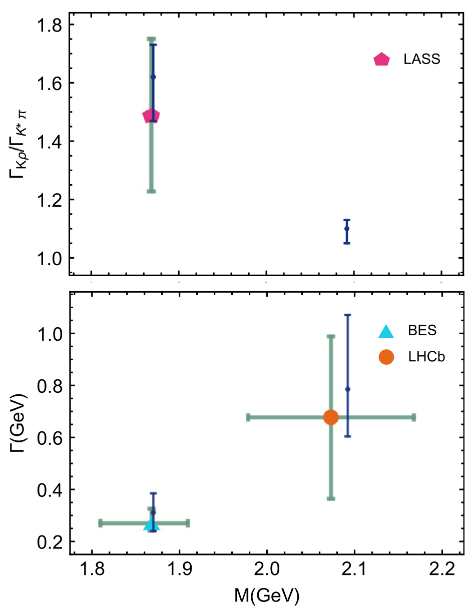

FIG. 2. Our theoretical results and the resonance parameters of $K_2^*(1980)$ measured by different experiments collected in PDG [1]. Here, the green lines with triangle and disk denote the central value of mass and decay width of $K_2^*(1980)$ measured by the BESIII Collaboration, respectively [3,4]. The green line with rose pentagon denotes the central value of decay-branching ratio of $K_2^*(1980)$ measured by the LASS Collaboration [2]. The purplish blue lines are our calculation results.

TABLE II. Allowed partial strong decay widths of 2^3P_2 and 1^3F_2 state.

Decay channels	2^3P_2	1^3F_2
Kb_1	8.15–26.3	118–145
$K_1\pi$	12.4–33.8	104–152
Ka_1	4.3–13.8	61.8–79.8
$K^*\rho$	55.8–77.8	24.1–131
Kh_1	5.51–10.8	39.5–47.5
$K_2{}^*\pi$	15.2–28.3	18.9–34.4
Ka_2	0–25.9	14–32.4
Kf_1	0.23–3.2	15.7–25.1
$K^*\omega$	18.7–24.9	7.64–42.3
$K\rho$	31.6–33	19.1–21.5
$K^*(892)\pi$	18.1–21.8	16.8–20.1
$K\pi$	0.0117–1.17	13.9–19.5
$K(1460)\pi$	5.15–21.7	9.26–16.6
$Kf_2(1270)$	1.29–12.4	6.03–11.2
$K\omega$	10.5–11	6.43–7.19
$K\pi(1300)$	0–10.5	3.02–9.17
$K^*(1410)\pi$	15.2–46.7	3.37–5.7
$K^*\eta$	3.93–5.02	3.79–4.47
$K\eta$	0.361–0.801	3.77–4.4
$K\eta'$	0.632–0.818	2.31–3.27
$K_1'\pi$	12.5–16.9	0.113–0.498
$K_1\rho$	0	0–149
$K_1\eta$	0	24.3–37.9
$K\eta_2$	0	0–62.8
$K_1\omega$	0	0–48.1
K^*h_1	0	0–34.2
K^*b_1	0	0–61.4
K^*a_1	0	0–33.7
$K_2{}^*\eta$	0	0–4.99
$K^*\eta'$	0	0.319–2.45
$K_3{}^*(1780)\pi$	0	0.0372–7.77
$K^*(1680)\pi$	0	0.0562–3.73

The decay amplitude can be expressed in another form by the Jacob-Wick formula [62]:

$$\mathcal{M}^{JL}(\mathbf{P}) = \frac{\sqrt{4\pi(2L+1)}}{2J_A+1} \sum_{M_{J_B} M_{J_C}} \langle L0; JM_{J_A}|J_A M_{J_A}\rangle \times \langle J_B M_{J_B}; J_C M_{J_C}|J_A M_{J_A}\rangle \mathcal{M}^{M_{J_A} M_{J_B} M_{J_C}}. \quad (19)$$

Then, the general decay width will be

$$\Gamma = \frac{\pi}{4} \frac{|\mathbf{P}|}{m_A^2} \sum_{J,L} |\mathcal{M}^{JL}(\mathbf{P})|^2, \quad (20)$$

where m_A is the mass of an initial state A. In our calculation, the spatial wave functions for the mesons are given in Ref. [19]. The value of γ is 11.6.

B. Mass spectrum analysis

In Table I, we give the mass spectrum for the K_2^* mesons by using different models. We can see from our previous work (Ref. [63]) that the ground state of $K_2^*(1P)$ has a mass of 1432 MeV, which is close to the result obtained from the experimental data [1]. For the highly excited states of the P-wave K_2^* mesons, $K_2^*(2P)$, $K_2^*(3P)$, and $K_2^*(4P)$ have masses of 1870, 2198, and 2438 MeV, respectively, which are smaller than those reported in Ref. [7]. For the F-wave K_2^*, $K_2^*(1F)$ is predicted to have a mass of 2092 MeV, which is similar to the value of $2073 \pm 94^{+245}_{-240}$ obtained from the LHCb data in Ref. [4]. $K_2^*(2F)$ has a mass of 2356 MeV and $K_2^*(3F)$ has a mass of 2552 MeV, which are both smaller than that reported in Ref. [7]. Additionally, the results of $K_2^*(1P)$, $K_2^*(2P)$, and $K_2^*(1F)$ in Ref. [64] are also close to the experimental data.

III. TWO-BODY STRONG DECAY ANALYSIS

A. The 2^3P_2 and 1^3F_2 states of K_2^*

When we use the experimental values $1868 \pm 8^{+40}_{-57}$ MeV and 2073 ± 94 MeV [here, we do not take into account the large systematic error in $K_2^*(2070)$] as inputs for the mass of 2^3P_2 and 1^3F_2 states. The QPC model provides an effective approach for determining the decay widths for the 2^3P_2 and 1^3F_2 states, which have values of 285 ± 45 and 855 ± 225 MeV, respectively. To clearly compare our prediction with the resonance parameters of $K_2^*(1980)$ measured by different experiments collected in PDG [1], we present the total width and decay-branching ratio for $K_2^*(1870)$ and $K_2^*(2070)$ with the variation of the mass. A comparison of our theoretical result for the total width of $K_2^*(1870)$ with experimental data is shown by the lower diagram in Fig. 2; note that our result is very close to the BESIII experimental data [3] marked by the green line with triangle in Fig. 2. Based on the decay-branching ratio of $\frac{K\rho}{K^*\pi}$, when $K_2^*(1870)$ was regarded as a 2^3P_2 state, our result

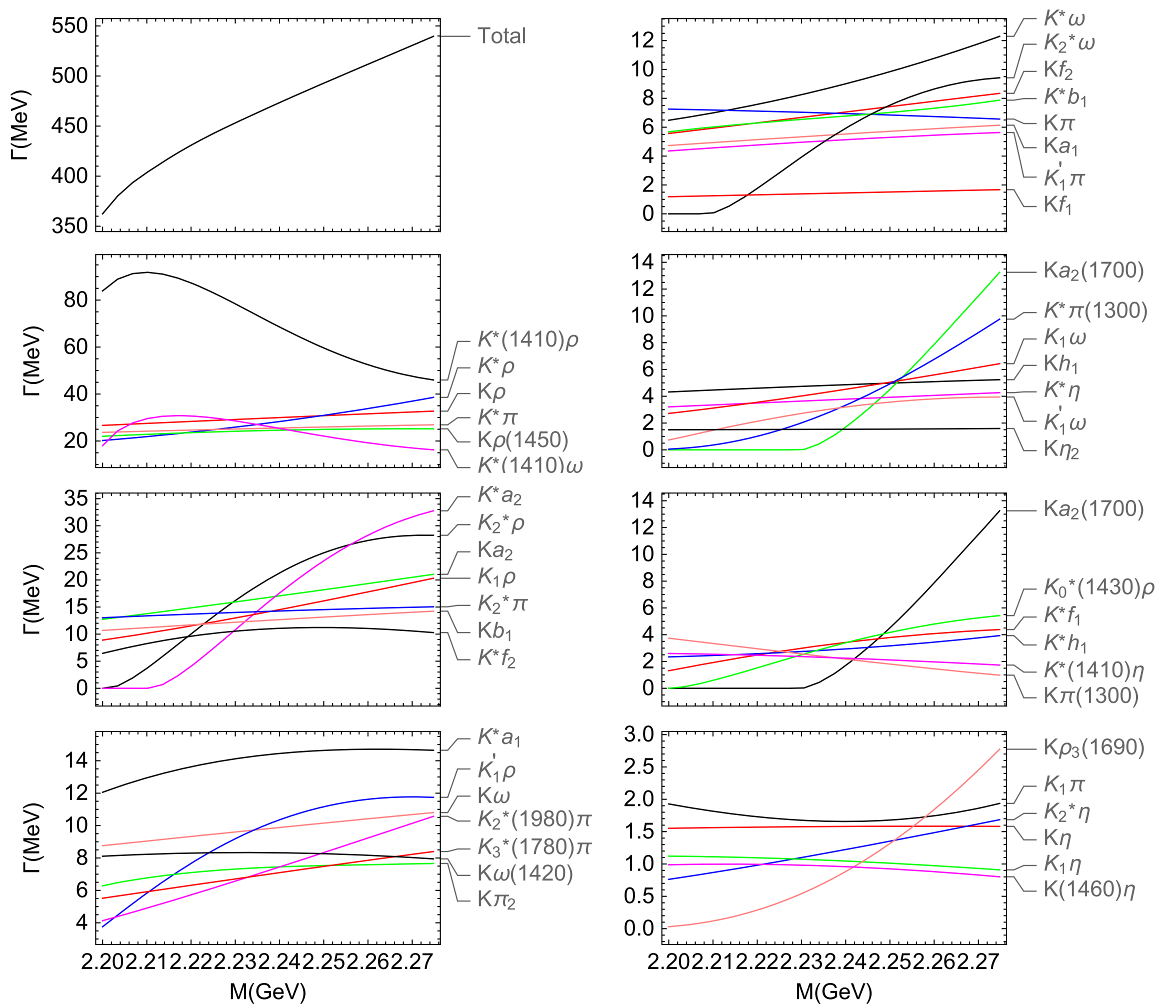

FIG. 3. M dependence of the calculated decay widths of 3^3P_2 state.

of $\frac{\Gamma_{K\rho}}{\Gamma_{K^*\pi}} = 1.62^{+0.11}_{-0.15}$ conforms well to the experimental value, $\frac{\Gamma_{K\rho}}{\Gamma_{K^*\pi}} = 1.49 \pm 0.24 \pm 0.09$ [2]. Thus, explaining $K_2^*(1870)$ as a 2^3P_2 state is further tested through the decay-branching ratio of $\frac{K\rho}{K^*\pi}$. In the upper diagram of Fig. 2, when we treat $K_2^*(2070)$ as the 1F state, the ratio of $\frac{\Gamma_{K\rho}}{\Gamma_{K^*\pi}}$ is approximately 1.05–1.13. The width has an overlap with the LHCb data $\Gamma_{K_2^*(2070)} = 678 \pm 311^{+559}_{-1153}$ MeV in the $M = (1979\text{–}2167)$ MeV range ($M_{K_2^*(2070)} = 2073 \pm 94^{+245}_{-240}$ MeV [4]). The total error $+640$ MeV is comparable with the center width of 678 MeV, and another total error -1194 MeV is nearly two times this center width value, which is the largest experimental error for the experimental data obtained for the K meson family in PDG [1]. Note that the mass and width of the $K^*(2^+)2^3P_2$ state are fitted using the quantum numbers $n^{2S+1}L_J = 2^3P_2$ in Ref. [4]. Additionally, we also note that PDG edition 2022 does not adopt these LHCb data [66]; perhaps this "nonadoption" can be attributed to the large error. Therefore, we suggest that experimenters add the $K_2^*(1^3F_2)$ state in the fit scheme reported in [4], which makes it possible to reduce the experimental error of K_2^*.

We have a nice description of $K_2^*(1870)$ for the mass spectrum and decay behaviors under the assignment of K_2^* (2^3P_2). The assignment of K_2^* (1^3F_2) for $K_2^*(2070)$ requires more experimental support. We hope our theoretical result can help to establish this $K_2^*(1F)$ state.

The two-body decay information for the 2^3P_2 and 1^3F_2 states is shown in Table II. Kb_1, $K_1\pi$, Ka_1, and $K^*\rho$ all make important contributions to the 2^3P_2 and 1^3F_2 states. The decay modes $K_1\rho$, $K_1\eta$, $K_1\eta_2$, and $K_1\omega$ are predicted to be dominant to 1^3F_2 state, but has no contribution to 2^3P_2 state. Kh_1, $K_2^*\pi$, Ka_2, Kf_1, $K^*\omega$, $K\rho$, and $K^*\pi$ have visible contribution to the total width of 2^3P_2 and 1^3F_2 state. $K^*\eta'$, $K_3^*(1780)\pi$, and $K^*(1680)\pi$ have very small widths in the final states of the 2^3P_2 and 1^3F_2 states. The SPEC experiment found an indication of a decay channel for $K_2^*(1980)$: $Kf_2(1270)$ in 2003 [67]. The PDG considers only $K\rho$, $K^*\pi$, $Kf_2(1270)$, $K^*\phi$ modes for

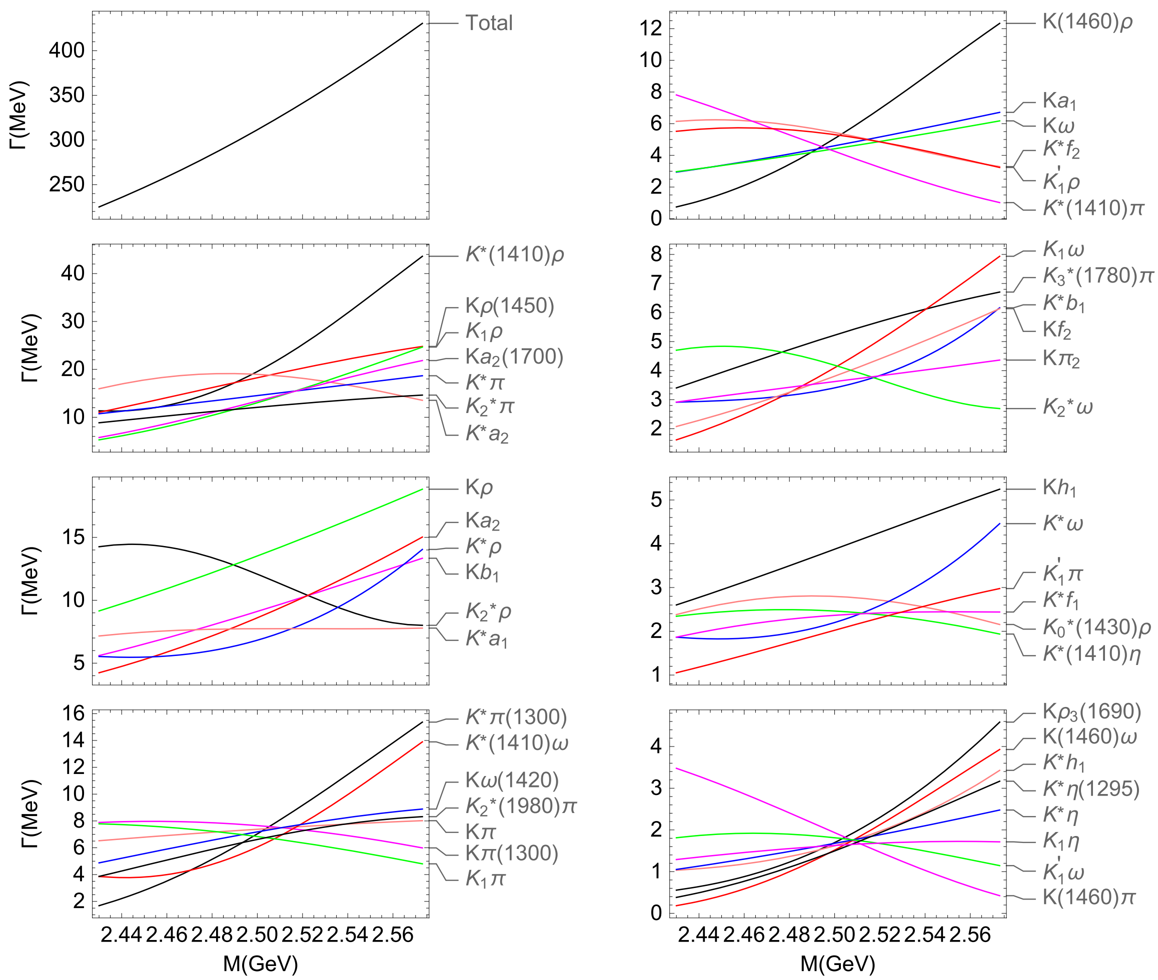

FIG. 4. M dependence of the calculated decay widths of 4^3P_2 state.

"$K_2^*(1980)(2P)$" state, and $K_2^*(1980) \to K\eta$ was observed for the first time by Chen *et al.* in the $D_0 \to K^-\pi^+$ decays [68]. The width of the $Kf_2(1270)$ channel is predicted to be 1.29–12.4 and 6.03–11.2 MeV for the 2^3P_2 and 1^3F_2 states, respectively. The predicted ordering of two widths $K\rho > K^*\pi$ is in agreement with experiment [2], and the predicted and observed decay-branching ratios are roughly consistent with each other.

The largest channels for the 1^3F_2 state are predicted to be $K_1\rho$, Kb_1, $K^*\rho$, $K_1\pi$, and Ka_1, with branching fractions of 1, 7, 3, 7, and 4%, respectively, for $M = 2070$ MeV. Two of these channels are larger than 5%: Kb_1 and $K_1\pi$. Note that some decay channels have a strong dependence on the change in the mass, such as $K^*(1680)\pi$, $K^*\eta'$, $K(1460)\eta$, $K\eta(1295)$, $Kf_1(1420)$, and $K^*(1410)\eta$. Observation of these channels like $K\rho$, $K^*\pi$ and $K\pi$ can provide useful information about the nature of the $K_2^*(1980)$ meson.

B. Predicted $K_2^*(3P)$ and $K_2^*(4P)$ states

When further discussing the decay behavior of the 3^3P_2 state of the K_2^* meson family, we can estimate the total decay width of $K_2^*(3P)$ to be (360–540) MeV and the mass to be (2200–2276) MeV. The predicted main decay channels of $K_2^*(3P)$ include $K^*(1410)\rho$, $K^*\rho$, $K\rho$, $K^*\pi$, $K\rho(1450)$, and the $K^*(1410)\rho$ channel has a regnant position. The $K_1\pi$, $K_2^*\eta$, $K\eta$, $K_1\eta$, and $K(1460)\eta$ channels make very small contributions to the total decay, and they are not sensitive to the change in the mass. More details can be found in Fig. 3.

The calculated total decay width for $K_2^*(4P)$ is (225–430) MeV when taking $M = (2436–2566)$ MeV. It is evident from Fig. 4 that when searching for these decay modes, we find that only a few channels have branching fractions larger than a few percent. $K^*(1410)\rho$, $K\rho(1450)$, $K_1\rho$, $Ka_2(1700)$, $K^*\pi$, $K_2^*\pi$, and K^*a_2 are the main decay modes of the $K_2^*(4P)$, which have branching ratios of 0.04–0.10, 0.04–0.06, 0.03–0.06, 0.03–0.05, 0.04, 0.03–0.04, and 0.03–0.07, respectively.

C. Predicted $K_2^*(2F)$ and $K_2^*(3F)$ states

The predicted mass for the 2^3F_2 state in the K_2^* meson family is 2415 MeV. Our result (Fig. 5) shows that when we take the mass to range from 2355 to 2565 MeV, the

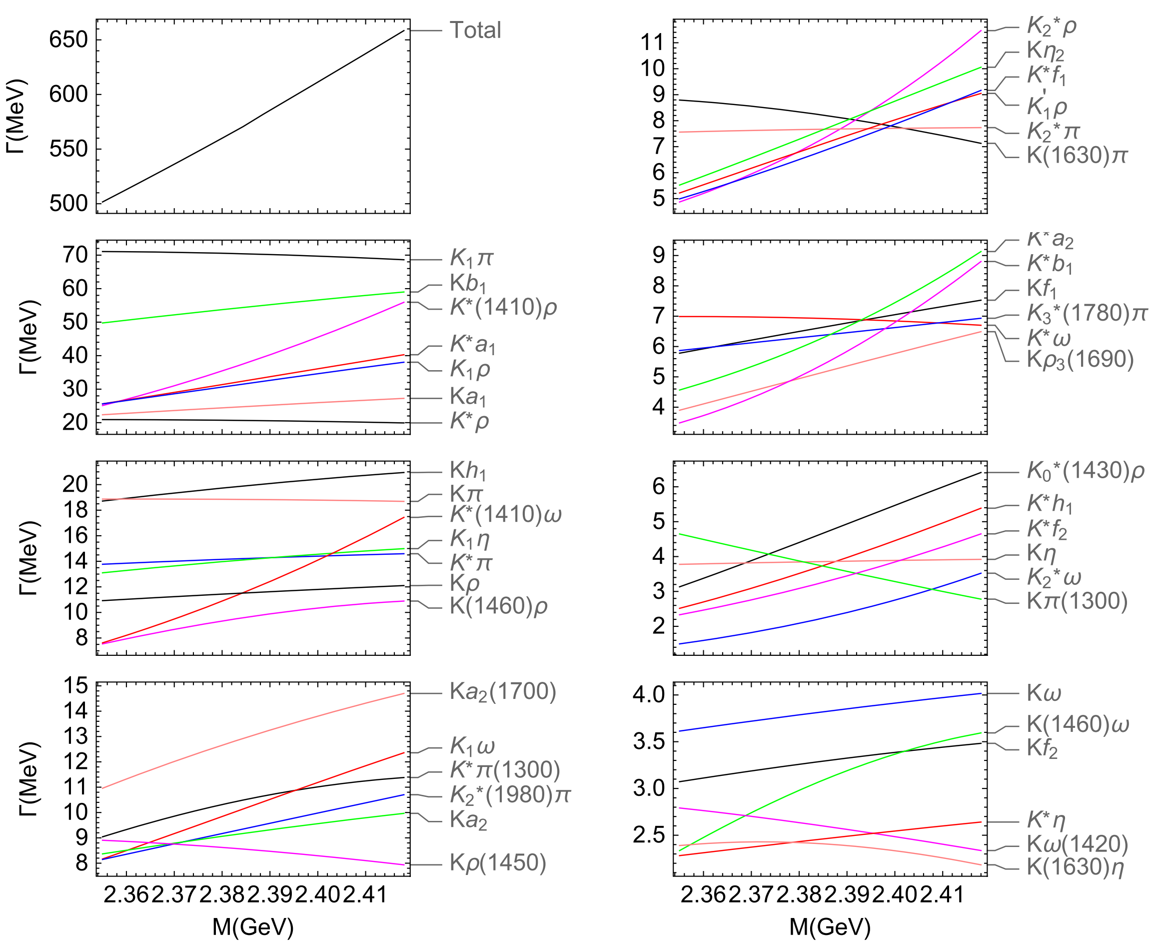

FIG. 5. M dependence of the calculated decay widths of 2^3F_2 state.

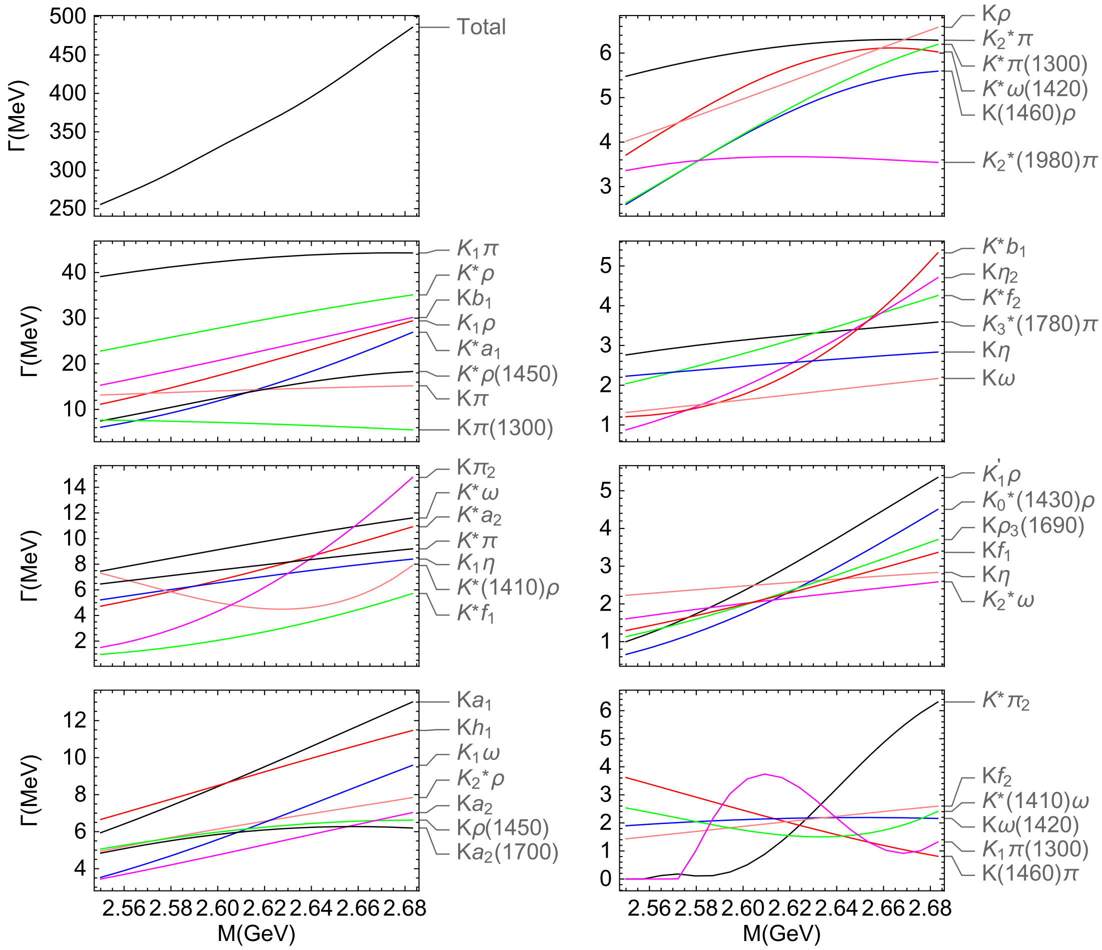

FIG. 6. M dependence of the calculated decay widths of 3^3F_2 state.

total width is $\Gamma_{K_2^*(2^3F_2)} = 580 \pm 80$ MeV. The largest decay channel $K_1\pi$ does not change significantly in the mass of $M = (2355\text{–}2565)$ MeV, and its branch ratio is approximately 0.12. The important decay channels are Kb_1, $K^*(1410)\rho$, K^*a_1, $K_1\rho$, Ka_1, and $K^*\rho$. In addition, Kh_1, $K\pi$, $K^*(1410)\omega$, $K_1\eta$, $K^*\pi$, $K\rho$, and $K(1460)\rho$ also make certain contributions. $K\omega$, $K(1460)\omega$, Kf_2, $K^*\eta$, $K\omega(1420)$, and $K(1630)\eta$ make small contributions. We consider that the predicted behavior of $K_2^*(2F)$ will be helpful for the experimental search for $K_2^*(2F)$ state.

As we can observe from Fig. 6, compared to the predicted $K_2^*(1F)$ state, the predicted $K_2^*(2F)$ state and $K_2^*(3F)$ state have more decay channels. The obtained mass is $M_{3^3F_2} = 2624 \pm 58$ MeV. The corresponding total decay width is approximately $\Gamma_{3^3F_2} = 370 \pm 120$ MeV. Note that the important decays are again distributed over several modes, and the larger decay modes are $K_1\pi$, $K^*\rho$, Kb_1, $K_1\rho$, K^*a_1, $K^*\rho(1450)$, $K\pi$, and $K\pi(1300)$. Kf_2, $K^*(1410)\omega$, $K\omega(1420)$, $K_1\pi(1300)$, and $K(1460)\pi$ contribute very little to the total decay width of $K_2^*(3F)$.

IV. CONCLUSION

The observed $K_2^*(1870)$ and $K_2^*(2070)$ are first described as 2^3P_2 and 1^3F_2 states, respectively. By analyzing the mass spectra obtained for the P-wave and F-wave K_2^* meson family and calculating the two-body strong decay for these two states, we find that our predicted results for $K_2^*(1870)$ are consistent with existing experimental findings. Our results about $K_2^*(2070)$ have a large overlap with existing experimental findings. Our theoretical results show that, $K_2^*(1870)$ can be regard as a 2^3P_2 state based on comparison with the experimental data. $K_2^*(2070)$ is likely to be a 1^3F_2 state. The 1^3F_2 state can have a relatively large width of 855 ± 225 MeV, and the ratio of $\frac{\Gamma_{K\rho}}{\Gamma_{K^*\pi}}$ is 1.05–1.13. Because of our explanations of $K_2^*(1870)$ and $K_2^*(2070)$, the spectroscopy for the P-wave and F-wave K_2^* mesons becomes abundant. Additionally, we predict the decay behaviors for the $K_2^*(2P)$ and $K_2^*(1F)$ states and the decay widths of channels such as $K\rho$, $K^*\pi$, and $Kf_2(1270)$ are calculated. These findings are expected to be revealed in future experiments. In addition to the 2^3P_2 and 1^3F_2 strange mesons, the decay behaviors for the other higher excited K_2^* mesons is also predicted in the present work. The masses and widths for these predicted states provide some basic information that will help in the search for these strange mesons in future experiments.

In addition, we hope that the resonance parameter (total width) for $K_2^*(2070)$ can be fitted again by the experimental group considering the quantum numbers $n^{2S+1}L_J = 1^3F_2$ for K_2^*, which will provide a powerful criterion for testing information to further confirm the $K_2^*(2070)$ state.

ACKNOWLEDGMENTS

This work is supported in part by National Natural Science Foundation of China under Grants No. 11965016 and No. 12247101, Qinghai Science and Technology Plan, Grant No. 2020-ZJ-728. C.-Q. P. thanks Jun-zhang Wang for the useful discussions.

T.-Y. L. and Y.-R. W. contributed equally to this work.

[1] P. Zyla *et al.* (Particle Data Group), Prog. Theor. Exp. Phys. **2020**, 083C01 (2020).
[2] D. Aston *et al.*, Nucl. Phys. **B292**, 693 (1987).
[3] M. Ablikim *et al.* (BESIII Collaboration), Phys. Rev. D **100**, 032004 (2019).
[4] R. Aaij *et al.* (LHCb Collaboration), Phys. Rev. D **95**, 012002 (2017).
[5] R. Aaij *et al.* (LHCb Collaboration), Phys. Rev. Lett. **127**, 082001 (2021).
[6] M. Ablikim *et al.* (BESIII Collaboration), Phys. Rev. D **101**, 032008 (2020).
[7] S. Godfrey and N. Isgur, Phys. Rev. D **32**, 189 (1985).
[8] E. Laermann, F. Langhammer, I. Schmitt, and P. M. Zerwas, Phys. Lett. B **173**, 437 (1986).
[9] K. D. Born, E. Laermann, N. Pirch, T. F. Walsh, and P. M. Zerwas, Phys. Rev. D **40**, 1653 (1989).
[10] F. Knechtli and R. Sommer (ALPHA Collaboration), Nucl. Phys. **B590**, 309 (2000).
[11] O. Philipsen and H. Wittig, Nucl. Phys. B, Proc. Suppl. **73**, 706 (1999).
[12] R.-C. Chen and X. Wu, Commun. Theor. Phys. **65**, 321 (2016).
[13] Y.-B. Ding, K.-T. Chao, and D.-H. Qin, Chin. Phys. Lett. **10**, 460 (1993).
[14] Y.-B. Ding, K.-T. Chao, and D.-H. Qin, Phys. Rev. D **51**, 5064 (1995).
[15] B.-Q. Li and K.-T. Chao, Phys. Rev. D **79**, 094004 (2009).
[16] M.-X. Duan and X. Liu, Phys. Rev. D **104**, 074010 (2021).
[17] Q.-T. Song, D.-Y. Chen, X. Liu, and T. Matsuki, Phys. Rev. D **91**, 054031 (2015).
[18] Q.-T. Song, D.-Y. Chen, X. Liu, and T. Matsuki, Phys. Rev. D **92**, 074011 (2015).
[19] C.-Q. Pang, Y.-R. Wang, and C.-H. Wang, Phys. Rev. D **99**, 014022 (2019).
[20] L. Micu, Nucl. Phys. **B10**, 521 (1969).
[21] A. Le Yaouanc, L. Oliver, O. Pene, and J. Raynal, Phys. Rev. D **8**, 2223 (1973).
[22] E. van Beveren, C. Dullemond, and G. Rupp, Phys. Rev. D **21**, 772 (1980); **22**, 787(E) (1980).
[23] E. van Beveren, G. Rupp, T. Rijken, and C. Dullemond, Phys. Rev. D **27**, 1527 (1983).
[24] A. Le Yaouanc, L. Oliver, O. Pene, and J. C. Raynal, *Hardron Transitions In The Quark Model* (Gordon and Breach, New York, USA, 1988).
[25] W. Roberts and B. Silvestre-Brac, Few Body Syst. **11**, 171 (1992).
[26] S. Capstick and W. Roberts, Phys. Rev. D **49**, 4570 (1994).
[27] H. G. Blundell and S. Godfrey, Phys. Rev. D **53**, 3700 (1996).
[28] E. Ackleh, T. Barnes, and E. Swanson, Phys. Rev. D **54**, 6811 (1996).
[29] S. Capstick and B. Keister, arXiv:nucl-th/9611055.
[30] R. Bonnaz, B. Silvestre-Brac, and C. Gignoux, Eur. Phys. J. A **13**, 363 (2002).
[31] F. Close and E. Swanson, Phys. Rev. D **72**, 094004 (2005).
[32] B. Zhang, X. Liu, W.-Z. Deng, and S.-L. Zhu, Eur. Phys. J. C **50**, 617 (2007).
[33] J. Lu, X.-L. Chen, W.-Z. Deng, and S.-L. Zhu, Phys. Rev. D **73**, 054012 (2006).
[34] Z.-F. Sun and X. Liu, Phys. Rev. D **80**, 074037 (2009).
[35] X. Liu, Z.-G. Luo, and Z.-F. Sun, Phys. Rev. Lett. **104**, 122001 (2010).
[36] Z.-F. Sun, J.-S. Yu, X. Liu, and T. Matsuki, Phys. Rev. D **82**, 111501 (2010).
[37] T. Rijken, M. Nagels, and Y. Yamamoto, Nucl. Phys. **A835**, 160 (2010).
[38] J.-S. Yu, Z.-F. Sun, X. Liu, and Q. Zhao, Phys. Rev. D **83**, 114007 (2011).
[39] Z.-Y. Zhou and Z. Xiao, Phys. Rev. D **84**, 034023 (2011).
[40] Z.-C. Ye, X. Wang, X. Liu, and Q. Zhao, Phys. Rev. D **86**, 054025 (2012).
[41] X. Wang, Z.-F. Sun, D.-Y. Chen, X. Liu, and T. Matsuki, Phys. Rev. D **85**, 074024 (2012).
[42] Y. Sun, X. Liu, and T. Matsuki, Phys. Rev. D **88**, 094020 (2013).
[43] L.-P. He, X. Wang, and X. Liu, Phys. Rev. D **88**, 034008 (2013).
[44] Y. Sun, Q.-T. Song, D.-Y. Chen, X. Liu, and S.-L. Zhu, Phys. Rev. D **89**, 054026 (2014).
[45] C.-Q. Pang, L.-P. He, X. Liu, and T. Matsuki, Phys. Rev. D **90**, 014001 (2014).

[46] B. Wang, C.-Q. Pang, X. Liu, and T. Matsuki, Phys. Rev. D **91**, 014025 (2015).
[47] K. Chen, C.-Q. Pang, X. Liu, and T. Matsuki, Phys. Rev. D **91**, 074025 (2015).
[48] E. van Beveren and G. Rupp, Phys. Rev. Lett. **91**, 012003 (2003).
[49] Y. R. Liu, X. Liu, and S. L. Zhu, Phys. Rev. D **79**, 094026 (2009).
[50] Y. B. Dai, X. Q. Li, S. L. Zhu, and Y. B. Zuo, Eur. Phys. J. C **55**, 249 (2008).
[51] W. Lucha, F. Schoberl, and D. Gromes, Phys. Rep. **200**, 127 (1991).
[52] A. Le Yaouanc, L. Oliver, O. Pene, and J.-C. Raynal, Phys. Rev. D **9**, 1415 (1974).
[53] A. Le Yaouanc, L. Oliver, O. Pene, and J. Raynal, Phys. Rev. D **11**, 1272 (1975).
[54] A. Le Yaouanc, L. Oliver, O. Pene, and J. Raynal, Phys. Lett. **72B**, 57 (1977).
[55] A. Le Yaouanc, L. Oliver, O. Pene, and J.-C. Raynal, Phys. Lett. **71B**, 397 (1977).
[56] P. R. Page, Nucl. Phys. **B446**, 189 (1995).
[57] A. I. Titov, T. I. Gulamov, and B. Kampfer, Phys. Rev. D **53**, 3770 (1996).
[58] H. G. Blundell, Meson properties in the quark model: A look at some outstanding problems, Other thesis, 1996, arXiv:hep-ph/9608473.
[59] H. Q. Zhou, R. G. Ping, and B. S. Zou, Phys. Lett. B **611**, 123 (2005).
[60] Z.-G. Luo, X.-L. Chen, and X. Liu, Phys. Rev. D **79**, 074020 (2009).
[61] J.-C. Feng, X.-W. Kang, Q.-F. Lü, and F.-S. Zhang, Phys. Rev. D **104**, 054027 (2021).
[62] M. Jacob and G. Wick, Ann. Phys. (N.Y.) **7**, 404 (1959).
[63] C.-Q. Pang, J.-Z. Wang, X. Liu, and T. Matsuki, Eur. Phys. J. C **77**, 861 (2017).
[64] D. Ebert, R. N. Faustov, and V. O. Galkin, Phys. Rev. D **79**, 114029 (2009).
[65] K. A. Olive *et al.* (Particle Data Group), Chin. Phys. C **38**, 090001 (2014).
[66] R. L. Workman *et al.* (Particle Data Group), Prog. Theor. Exp. Phys. **2022**, 083C01 (2022).
[67] G. D. Tikhomirov, I. A. Erofeev, O. N. Erofeeva, and V. N. Luzin, Phys. At. Nucl. **66**, 828 (2003).
[68] Y. Q. Chen *et al.* (Belle Collaboration), Phys. Rev. D **102**, 012002 (2020).